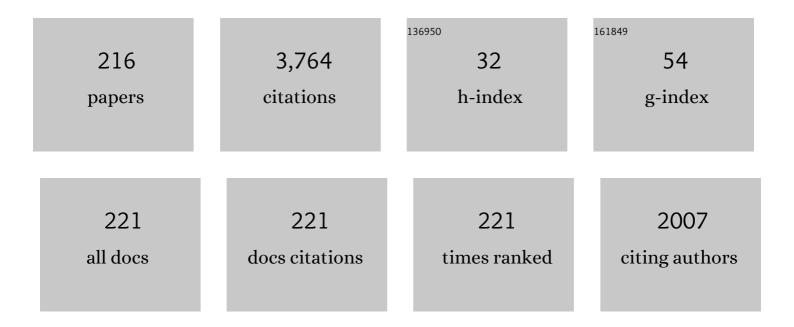
## Maxim Ryzhii

List of Publications by Year in descending order

Source: https://exaly.com/author-pdf/277757/publications.pdf Version: 2024-02-01



Μλνιμ Ρυζηιι

#	Article	IF	CITATIONS
1	Terahertz-wave generation using graphene: Toward new types of terahertz lasers. Proceedings of the IEEE, 2024, , 1-13.	21.3	1
2	Graphene-based plasmonic metamaterial for terahertz laser transistors. Nanophotonics, 2022, 11, 1677-1696.	6.0	15
3	Coulomb drag and plasmonic effects in graphene field-effect transistors enable resonant terahertz detection. Applied Physics Letters, 2022, 120, 111102.	3.3	3
4	Pacemaking function of two simplified cell models. PLoS ONE, 2022, 17, e0257935.	2.5	3
5	Modulation characteristics of uncooled graphene photodetectors. Journal of Applied Physics, 2021, 129, .	2.5	10
6	Heat capacity of nonequilibrium electron-hole plasma in graphene layers and graphene bilayers. Physical Review B, 2021, 103, .	3.2	2
7	xmins:mmi="http://www.w3.org/1998/Math/Wath/Wath/ML" display="inline" overflow="scroll"> <mml:msup><mml:mi>n</mml:mi><mml:mo>+</mml:mo></mml:msup> - <mml:math <br="" display="inline" xmlns:mml="http://www.w3.org/1998/Math/MathML">overflow="scroll"&gt;<mml:mi>i</mml:mi></mml:math> - <mml:math< td=""><td>3.8</td><td>18</td></mml:math<>	3.8	18
8	Coulomb electron drag mechanism of terahertz plasma instability in n+-i-n-n+ graphene FETs with ballistic injection. Applied Physics Letters, 2021, 119, .	3.3	13
9	Theoretical analysis of injection driven thermal light emitters based on graphene encapsulated by hexagonal boron nitride. Optical Materials Express, 2021, 11, 468.	3.0	8
10	Current Driven Plasma Instability in Graphene-FETs with Coulomb Electron Drag. , 2021, , .		0
11	Comparison of Responses of Ion-Channel and Simplified Pacemaker Cell Models on External Stimulation, 2021 Effect of Coulomb Carrier Drag and Terahertz Plasma Instability in <mml:math< td=""><td></td><td>0</td></mml:math<>		0
12	<pre>vmills.mm= mttp://www.w3.org/1998/Math/MathML oisplay= mme overflow="scroll"&gt;<mml:msup><mml:mi>p</mml:mi><mml:mo>+</mml:mo></mml:msup> - <mml:math <br="" display="inline" xmlns:mml="http://www.w3.org/1998/Math/MathML">overflow="scroll"&gt;<mml:mi>p</mml:mi></mml:math> - <mml:math< pre=""></mml:math<></pre>	3.8	8
13	xmlns:mml="http://www.w3.org/1998/Math/MathML" display="inline" overflow="scroll", xmml:mixix/m Sub-terahertz FET detector with self-assembled Sn-nanothreads. Journal Physics D: Applied Physics, 2020, 53, 075102.	2.8	7
14	Simulation of the Effect of AC stimulation on Atrioventricular Node with Nonlinear Model. , 2020, , .		0
15	Multiple graphene-layer-based heterostructures with van der Waals barrier layers for terahertz superluminescent and laser diodes with lateral/vertical current injection. Semiconductor Science and Technology, 2020, 35, 085023.	2.0	3
16	Far-infrared photodetectors based on graphene/black-AsP heterostructures. Optics Express, 2020, 28, 2480.	3.4	27
17	Far-infrared and terahertz emitting diodes based on graphene/black-P and graphene/MoS2 heterostructures. Optics Express, 2020, 28, 24136.	3.4	7
18	Far-infrared photodetection in graphene nanoribbon heterostructures with black-phosphorus base layers. Optical Engineering, 2020, 60, .	1.0	1

#	Article	IF	CITATIONS
19	Concepts of infrared and terahertz photodetectors based on vertical graphene van der Waals and HgTe-CdHgTe heterostructures. Opto-electronics Review, 2019, 27, 219-223.	2.4	2
20	Negative terahertz conductivity and amplification of surface plasmons in graphene–black phosphorus injection laser heterostructures. Physical Review B, 2019, 100, .	3.2	21
21	Characteristics of vertically stacked graphene-layer infrared photodetectors. Solid-State Electronics, 2019, 155, 123-128.	1.4	1
22	Negative photoconductivity and hot-carrier bolometric detection of terahertz radiation in graphene-phosphorene hybrid structures. Journal of Applied Physics, 2019, 125, 151608.	2.5	12
23	Optical Pumping of Graphene-Based Heterostructures with Black-Arsenic-Phosphorus Absorbing-Cooling Layer for Terahertz Lasing. , 2019, , .		Ο
24	Optimization of Dual Pathway AV Nodal Conduction Model. Journal of Physics: Conference Series, 2019, 1372, 012078.	0.4	3
25	Negative Terahertz Conductivity at Vertical Carrier Injection in a Black-Arsenic-Phosphorus–Graphene Heterostructure Integrated With a Light-Emitting Diode. IEEE Journal of Selected Topics in Quantum Electronics, 2019, 25, 1-9.	2.9	4
26	Terahertz photoconductive emitter with dielectric-embedded high-aspect-ratio plasmonic grating for operation with low-power optical pumps. AIP Advances, 2019, 9, .	1.3	43
27	Optical pumping in graphene-based terahertz/far-infrared superluminescent and laser heterostructures with graded-gap black-PxAs1â^'x absorbing-cooling layers. Optical Engineering, 2019, 59, 1.	1.0	8
28	Negative and positive terahertz and infrared photoconductivity in uncooled graphene. Optical Materials Express, 2019, 9, 585.	3.0	24
29	Optical pumping through a black-As absorbing-cooling layer in graphene-based heterostructure: thermo-diffusion model. Optical Materials Express, 2019, 9, 4061.	3.0	9
30	Graphene-based 2D-heterostructures for terahertz lasers and amplifiers. , 2019, , .		1
31	Plasmonic terahertz emitters with high-aspect ratio metal gratings. , 2019, , .		0
32	Vertical Hot-electron Terahertz Detectors Based on Black-As1?xPx/graphene/black-As1?yPy Heterostructures. Sensors and Materials, 2019, 31, 2271.	0.5	2
33	Lateral terahertz hot-electron bolometer based on an array of Sn nanothreads in GaAs. Journal Physics D: Applied Physics, 2018, 51, 135101.	2.8	17
34	Comparison of Intersubband Quantum-Well and Interband Graphene-Layer Infrared Photodetectors. IEEE Journal of Quantum Electronics, 2018, 54, 1-8.	1.9	9
35	Device model for pixelless infrared image up-converters based on polycrystalline graphene heterostructures. Journal of Applied Physics, 2018, 123, 014503.	2.5	3
36	Terahertz light-emitting graphene-channel transistor toward single-mode lasing. Nanophotonics, 2018, 7, 741-752.	6.0	57

#	Article	IF	CITATIONS
37	Development of Simplified Model of Atrioventricular Node with Dual Pathway. , 2018, , .		5
38	Plasmonic terahertz antennas with high-aspect ratio metal gratings. EPJ Web of Conferences, 2018, 195, 02009.	0.3	2
39	Sn-nanothreads in GaAs matrix and their sub- and terahertz applications. Journal of Physics: Conference Series, 2018, 1092, 012166.	0.4	5
40	Cardiac Conduction Model for Generating 12 Lead ECG Signals With Realistic Heart Rate Dynamics. IEEE Transactions on Nanobioscience, 2018, 17, 525-532.	3.3	39
41	Electrical modulation of terahertz radiation using graphene-phosphorene heterostructures. Semiconductor Science and Technology, 2018, 33, 124010.	2.0	19
42	Real-space-transfer mechanism of negative differential conductivity in gated graphene-phosphorene hybrid structures: Phenomenological heating model. Journal of Applied Physics, 2018, 124, 114501.	2.5	15
43	Interband infrared photodetectors based on HgTe–CdHgTe quantum-well heterostructures. Optical Materials Express, 2018, 8, 1349.	3.0	13
44	Quasiperiodicity route to chaos in cardiac conduction model. Communications in Nonlinear Science and Numerical Simulation, 2017, 42, 370-378.	3.3	17
45	Infrared photodetectors based on graphene van der Waals heterostructures. Infrared Physics and Technology, 2017, 84, 72-81.	2.9	17
46	Dynamic Conductivity and Two-Dimensional Plasmons in Lateral CNT Networks. International Journal of High Speed Electronics and Systems, 2017, 26, 1740004.	0.7	0
47	Current-injection terahertz lasing in a distributed-feedback dual-gate graphene-channel transistor. Proceedings of SPIE, 2017, , .	0.8	0
48	Dynamic Conductivity and Two-Dimensional Plasmons in Lateral CNT Networks. Selected Topics in Electornics and Systems, 2017, , 109-118.	0.2	0
49	Infrared detection and photon energy up-conversion in graphene layer infrared photodetectors integrated with LEDs based on van der Waals heterostructures: Concept, device model, and characteristics. Infrared Physics and Technology, 2017, 85, 307-314.	2.9	3
50	Effect of doping on the characteristics of infrared photodetectors based on van der Waals heterostructures with multiple graphene layers. Journal of Applied Physics, 2017, 122, .	2.5	12
51	Terahertz LED based on current injection dual-gate graphene-channel field effect transistors. , 2017, , .		0
52	Detection and up-conversion of infrared radiation using van der Waals heterostructures with graphene layers. , 2017, , .		0
53	Terahertz light emitting transistor based on current injection dualgate graphene-channel FET. , 2017, ,		0
54	Nonlinear response of infrared photodetectors based on van der Waals heterostructures with graphene layers. Optics Express, 2017, 25, 5536.	3.4	18

#	Article	IF	CITATIONS
55	Broadband Terahertz-Light Emission by Current-Injection Distributed-Feedback Dual-Gate Graphene-Channel Field-Effect Transistor. , 2017, , .		1
56	Plasmonic Enhancement of Terahertz Devices Efficiency. , 2017, , .		0
57	TERAHERTZ AND INFRARED PHOTODETECTORS BASED ON VERTICAL GRAPHENE VAN DER WAALS HETEROSTRUCTURES: CONCEPTS, FEATURES OF OPERATION AND CHARACTERISTICS. , 2017, , 159-167.		Ο
58	5.2-THz single-mode lasing in current-injection distributed-feedback dual-gate graphene-channel field-effect transistor. , 2016, , .		0
59	Plasmonic Enhancement of Terahertz Devices Efficiency. International Journal of High Speed Electronics and Systems, 2016, 25, 1640019.	0.7	Ο
60	Resonant plasmonic terahertz detection in graphene split-gate field-effect transistors with lateral p–n junctions. Journal Physics D: Applied Physics, 2016, 49, 315103.	2.8	27
61	Sn nanothreads in GaAs: experiment and simulation. Proceedings of SPIE, 2016, , .	0.8	Ο
62	Simulink heart model for simulation of the effect of external signals. , 2016, , .		1
63	Two-dimensional plasmons in lateral carbon nanotube network structures and their effect on the terahertz radiation detection. Journal of Applied Physics, 2016, 120, 044501.	2.5	18
64	Graphene-based van der Waals heterostructures for emission and detection of terahertz radiation. Proceedings of SPIE, 2016, , .	0.8	2
65	Single-mode terahertz emission from current-injection graphene-channel transistor under population inversion. , 2016, , .		Ο
66	Models for plasmonic THz detectors based on graphene split-gate FETs with lateral p-n junctions. , 2016, , .		0
67	Current-Injection Terahertz Lasing in Distributed-Feedback Dual-Gate Graphene-Channel Field-Effect Transistor. , 2016, , .		0
68	Resonant plasmonic terahertz detection in vertical graphene-base hot-electron transistors. Journal of Applied Physics, 2015, 118, .	2.5	16
69	Negative terahertz conductivity in remotely doped graphene bilayer heterostructures. Journal of Applied Physics, 2015, 118, .	2.5	4
70	Graphene active plasmonics for terahertz device applications. , 2015, , .		0
71	Vertical hot-electron graphene-base transistors as resonant plasmonic terahertz detectors. , 2015, , .		0
72	Formation of second-degree atrioventricular blocks in the cardiac heterogeneous oscillator model. , 2015, 2015, 4491-4.		2

Maxim Ryzhii

#	Article	IF	CITATIONS
73	Graphene vertical cascade interband terahertz and infrared photodetectors. 2D Materials, 2015, 2, 025002.	4.4	20
74	Vertical electron transport in van der Waals heterostructures with graphene layers. Journal of Applied Physics, 2015, 117, 154504.	2.5	11
75	Recent advances in the research toward graphene-based terahertz lasers. , 2015, , .		4
76	Terahertz Wave Generation Using Graphene and Compound Semiconductor Nano-Heterostructures. Nanostructure Science and Technology, 2015, , 237-261.	0.1	0
77	Electron Capture in van der Waals Graphene-Based Heterostructures with WS <sub>2</sub> Barrier Layers. Journal of the Physical Society of Japan, 2015, 84, 094703.	1.6	18
78	S7-N2: Terahertz lasing and detection in double-graphene-layer structures. , 2014, , .		0
79	Effect of coupling on the pacemaker synchronization in coupled oscillator ECG model. , 2014, , .		3
80	Graphene vertical hot-electron terahertz detectors. Journal of Applied Physics, 2014, 116, 114504.	2.5	18
81	Double injection, resonant-tunneling recombination, and current-voltage characteristics in double-graphene-layer structures. Journal of Applied Physics, 2014, 115, .	2.5	18
82	Double graphene-layer structures for adaptive devices. , 2014, , .		0
83	Graphene plasmonic heterostructures for new types of terahertz lasers. , 2014, , .		0
84	A heterogeneous coupled oscillator model for simulation of ECG signals. Computer Methods and Programs in Biomedicine, 2014, 117, 40-49.	4.7	38
85	Voltage-tunable terahertz and infrared photodetectors based on double-graphene-layer structures. Applied Physics Letters, 2014, 104, .	3.3	32
86	Terahertz emission and detection in double-graphene-layer structures. , 2014, , .		1
87	Challenges to create graphene terahertz lasers. Journal of Physics: Conference Series, 2014, 486, 012007.	0.4	1
88	Self-consistent surface charges and electric field in p-i-n tunneling transit-time diodes based on single- and multiple-layer graphene structures. Journal of Physics: Conference Series, 2014, 486, 012011.	0.4	0
89	Plasma resonant terahertz photomixers based on double graphene layer structures. Journal of Physics: Conference Series, 2014, 486, 012032.	0.4	1
90	Bioradiolocation: Methods and Applications. Communications in Computer and Information Science, 2014, , 10-28.	0.5	2

#	Article	IF	CITATIONS
91	Modeling of Heartbeat Dynamics with a System of Coupled Nonlinear Oscillators. Communications in Computer and Information Science, 2014, , 67-75.	0.5	8
92	Double injection in graphene p-i-n structures. Journal of Applied Physics, 2013, 113, 244505.	2.5	32
93	Dynamic effects in double graphene-layer structures with inter-layer resonant-tunnelling negative conductivity. Journal Physics D: Applied Physics, 2013, 46, 315107.	2.8	46
94	Injection terahertz laser using the resonant inter-layer radiative transitions in double-graphene-layer structure. Applied Physics Letters, 2013, 103, .	3.3	47
95	Effect of self-consistent electric field on characteristics of graphene p-i-n tunneling transit-time diodes. Journal of Applied Physics, 2013, 113, .	2.5	10
96	Emission and Detection of Terahertz Radiation Using Two-Dimensional Electrons in Ill–V Semiconductors and Graphene. IEEE Transactions on Terahertz Science and Technology, 2013, 3, 63-71.	3.1	98
97	Graphene terahertz uncooled bolometers. Journal Physics D: Applied Physics, 2013, 46, 065102.	2.8	38
98	Concept of infrared photodetector based on graphene–graphene nanoribbon structure. Infrared Physics and Technology, 2013, 59, 137-141.	2.9	7
99	Terahertz-Wave Generation Using Graphene: Toward New Types of Terahertz Lasers. IEEE Journal of Selected Topics in Quantum Electronics, 2013, 19, 8400209-8400209.	2.9	68
100	Terahertz photomixing using plasma resonances in double-graphene layer structures. Journal of Applied Physics, 2013, 113, .	2.5	47
101	Double-graphene-layer terahertz laser: concept, characteristics, and comparison. Optics Express, 2013, 21, 31567.	3.4	34
102	Terahertz-wave generation using graphene: toward the creation of graphene injection lasers. , 2013, , .		0
103	GRAPHENE TUNNELING TRANSIT-TIME DIODES: CONCEPT, CHARACTERISTICS, AND ULTIMATE PERFORMANCE. , 2013, , .		0
104	Terahertz graphene lasers: Injection versus optical pumping. , 2013, , .		2
105	Graphene Terahertz Lasers: Injection versus Optical Pumping. Materials Research Society Symposia Proceedings, 2013, 1505, 1.	0.1	0
106	Terahertz-wave generation using graphene. Materials Research Society Symposia Proceedings, 2012, 1437, 36.	0.1	0
107	Effect of plasma resonances on dynamic characteristics of double graphene-layer optical modulator. Journal of Applied Physics, 2012, 112, .	2.5	50
108	Double graphene-layer plasma resonances terahertz detector. Journal Physics D: Applied Physics, 2012, 45, 302001.	2.8	76

#	Article	IF	CITATIONS
109	Terahertz wave generation using graphene — Toward the creation of terahertz graphene injection lasers. , 2012, , .		0
110	Graphene-based devices in terahertz science and technology. Journal Physics D: Applied Physics, 2012, 45, 303001.	2.8	234
111	Population inversion and terahertz lasing in graphene. Proceedings of SPIE, 2012, , .	0.8	0
112	Graphene materials and devices in terahertz science and technology. MRS Bulletin, 2012, 37, 1235-1243.	3.5	30
113	Terahertz and infrared photodetectors based on multiple graphene layer and nanoribbon structures. Opto-electronics Review, 2012, 20, .	2.4	53
114	Graphene-based electro-optical modulator: Concept and analysis. , 2012, , .		1
115	Effect of Heating and Cooling of Photogenerated Electron–Hole Plasma in Optically Pumped Graphene on Population Inversion. Japanese Journal of Applied Physics, 2011, 50, 094001.	1.5	35
116	Concepts of terahertz and infrared devices based on graphene structures. , 2011, , .		0
117	Analytical device model for graphene bilayer field-effect transistors using weak nonlocality approximation. Journal of Applied Physics, 2011, 109, 064508.	2.5	11
118	Toward the creation of terahertz graphene injection laser. Journal of Applied Physics, 2011, 110, .	2.5	141
119	Optical Excitation of Graphene, Population Inversion, and Terahertz Lasing. AIP Conference Proceedings, 2011, , .	0.4	0
120	Terahertz and infrared detectors based on graphene structures. Infrared Physics and Technology, 2011, 54, 302-305.	2.9	32
121	Tunneling recombination in optically pumped graphene with electron-hole puddles. Applied Physics Letters, 2011, 99, .	3.3	10
122	Terahertz light amplification of stimulated emission of radiation in optically pumped graphene. , 2011, ,		0
123	Characteristics of p–i–n Terahertz and Infrared Photodiodes Based on Multiple Graphene Layer Structures. Japanese Journal of Applied Physics, 2011, 50, 070117.	1.5	9
124	Characteristics of p–i–n Terahertz and Infrared Photodiodes Based on Multiple Graphene Layer Structures. Japanese Journal of Applied Physics, 2011, 50, 070117.	1.5	10
125	Effect of Heating and Cooling of Photogenerated Electron–Hole Plasma in Optically Pumped Graphene on Population Inversion. Japanese Journal of Applied Physics, 2011, 50, 094001.	1.5	37
126	Negative terahertz dynamic conductivity in electrically induced lateral p–i–n junction in graphene. Physica E: Low-Dimensional Systems and Nanostructures, 2010, 42, 719-721.	2.7	9

#	Article	IF	CITATIONS
127	Electrically induced <mml:math <br="" xmlns:mml="http://www.w3.org/1998/Math/MathML">display="inline"&gt;<mml:mrow><mml:mi>n</mml:mi><mml:mtext>â^²</mml:mtext><mml:mi>i</mml:mi><mml: in multiple graphene layer structures. Physical Review B, 2010, 82, .</mml: </mml:mrow></mml:math>	mtex <b>3.2</b> â^'<	/mn <b>2le</b> mtext><
128	Observation of Amplified Stimulated Terahertz Emission in Optically Pumped Epitaxial Graphene Heterostructures. , 2010, , .		1
129	Terahertz and infrared photodetection using p-i-n multiple-graphene-layer structures. Journal of Applied Physics, 2010, 107, .	2.5	73
130	Graphene tunneling transit-time device with electrically induced p-i-n junction. , 2009, , .		0
131	Graphene under optical pumping: nonequilibrium distributions, population inversion, and terahertz lasing. Proceedings of SPIE, 2009, , .	0.8	0
132	Terahertz Laser with Optically Pumped Graphene Layers and Fabri–Perot Resonator. Applied Physics Express, 2009, 2, 092301.	2.4	77
133	Graphene bilayer field-effect phototransistor for terahertz and infrared detection. Physical Review B, 2009, 79, .	3.2	86
134	Feasibility of terahertz lasing in optically pumped epitaxial multiple graphene layer structures. Journal of Applied Physics, 2009, 106, .	2.5	125
135	Graphene Nanoribbon Phototransistor: Proposal and Analysis. Japanese Journal of Applied Physics, 2009, 48, 04C144.	1.5	34
136	Device model for graphene bilayer field-effect transistor. Journal of Applied Physics, 2009, 105, 104510.	2.5	40
137	Combined resonance and resonant detection of modulated terahertz radiation in a micromachined high-electron mobility transistor. Physica Status Solidi C: Current Topics in Solid State Physics, 2008, 5, 277-281.	0.8	6
138	Thermionic and tunneling transport mechanisms in graphene fieldâ€effect transistors. Physica Status Solidi (A) Applications and Materials Science, 2008, 205, 1527-1533.	1.8	22
139	Current-voltage characteristics of a graphene-nanoribbon field-effect transistor. Journal of Applied Physics, 2008, 103, .	2.5	42
140	Analysis of resonant detection of terahertz radiation in high-electron mobility transistor with a nanostring/carbon nanotube as the mechanically floating gate. Journal of Applied Physics, 2008, 104, .	2.5	15
141	Population inversion of photoexcited electrons and holes in graphene and its negative terahertz conductivity. Physica Status Solidi C: Current Topics in Solid State Physics, 2008, 5, 261-264.	0.8	18
142	Tunneling Current–Voltage Characteristics of Graphene Field-Effect Transistor. Applied Physics Express, 2008, 1, 013001.	2.4	24
143	Mechanism of self-excitation of terahertz plasma oscillations in periodically double-gated electron channels. Journal of Physics Condensed Matter, 2008, 20, 384207.	1.8	30
144	High-frequency properties of a graphene nanoribbon field-effect transistor. Journal of Applied Physics, 2008, 104, 114505.	2.5	15

#	Article	IF	CITATIONS
145	PLASMA WAVES IN TWO-DIMENSIONAL ELECTRON SYSTEMS AND THEIR APPLICATIONS. Selected Topics in Electornics and Systems, 2008, , 77-94.	0.2	1
146	Plasma waves in graphene-based heterostructures and their terahertz device applications. , 2007, , .		0
147	Injection and Population Inversion in Electrically Induced p–n Junction in Graphene with Split Gates. Japanese Journal of Applied Physics, 2007, 46, L151-L153.	1.5	104
148	PLASMA WAVES IN TWO-DIMENSIONAL ELECTRON SYSTEMS AND THEIR APPLICATIONS. International Journal of High Speed Electronics and Systems, 2007, 17, 521-538.	0.7	11
149	Electromechanical and plasma resonances in two-dimensional electron systems with mechanically floating gates. , 2007, , .		0
150	Detector of modulated terahertz radiation based on HEMT with mechanically floating gate. , 2007, , .		0
151	Resonant detection of modulated terahertz radiation in micromachined high-electron-mobility transistor. Applied Physics Letters, 2007, 90, 203503.	3.3	19
152	Negative dynamic conductivity of graphene with optical pumping. Journal of Applied Physics, 2007, 101, 083114.	2.5	331
153	Population inversion in electrically and optically pumped graphene. Physica E: Low-Dimensional Systems and Nanostructures, 2007, 40, 317-320.	2.7	4
154	Plasma effects in lateral Schottky junction tunneling transit-time terahertz oscillator. Journal of Physics: Conference Series, 2006, 38, 228-233.	0.4	13
155	Resonant Terahertz Photomixing in Integrated High-Electron-Mobility Transistor and Quantum-Well Infrared Photodetector Device. Japanese Journal of Applied Physics, 2006, 45, 3648-3651.	1.5	5
156	Modeling of plasma oscillations and terahertz photomixing in HEMT-like heterostructure with lateral Schottky junction. , 2005, 6039, 176.		0
157	Terahertz Photomixing in Heterostructure Device Based on Integration of High-Electron Mobility Transistor and Quantum-Well Infrared Photodetector. , 2005, , .		0
158	Effect of near-ballistic photoelectron transport on resonant plasma-assisted photomixing in high-electron mobility transistors. Semiconductor Science and Technology, 2004, 19, S74-S76.	2.0	5
159	Characteristics of a terahertz photomixer based on a high-electron mobility transistor structure with optical input through the ungated regions. Journal of Applied Physics, 2004, 95, 2084-2089.	2.5	65
160	Comparison of dark current, responsivity and detectivity in different intersubband infrared photodetectors. Semiconductor Science and Technology, 2004, 19, 8-16.	2.0	83
161	Analytical and computer models of terahertz HEMT photomixer. , 2004, , .		1
162	Electric-field and space-charge distributions in InAs/GaAs quantum-dot infrared photodetectors: ensemble Monte Carlo particle modeling. Microelectronics Journal, 2003, 34, 411-414.	2.0	11

ΜΑΧΙΜ ΒΥΖΗΙΙ

#	Article	IF	CITATIONS
163	<title>Quantum well and quantum dot infrared photodetectors: physics of operation and modeling</title> . , 2003, , .		1
164	Self-consistent model for quantum well infrared photodetectors with thermionic injection under dark conditions. Journal of Applied Physics, 2002, 92, 207-213.	2.5	26
165	Analysis of dual-band quantum well photodetectors. Journal of Applied Physics, 2002, 91, 5887-5891.	2.5	3
166	<title>Why QDIPs are still inferior to QWIPs: theoretical analysis</title> ., 2001, , .		5
167	Periodic electric-field and charge domains in multiple quantum well infrared photodetectors. Infrared Physics and Technology, 2001, 42, 249-257.	2.9	0
168	Comment on "Local responsivity in quantum well photodetectors―[J. Appl. Phys. 86, 7059 (1999)]. Journal of Applied Physics, 2001, 89, 6563-6564.	2.5	0
169	Self-organization in multiple quantum well infrared photodetectors. Semiconductor Science and Technology, 2001, 16, 202-208.	2.0	8
170	Ensemble Monte Carlo Particle Modeling of IngaAs/InP Uni-Traveling-Carrier Photodiodes. , 2001, , 312-315.		1
171	Comment on "Photoconductivity mechanism of quantum well infrared photodetectors under localized photoexcitation―[Appl. Phys. Lett. 73, 3432 (1998)]. Applied Physics Letters, 2000, 76, 4010-4011.	3.3	3
172	Monte Carlo particle modeling of electron transport and capture processes in AlGaAs/GaAs multiple quantum-well infrared photodetectors. Physica E: Low-Dimensional Systems and Nanostructures, 2000, 7, 120-123.	2.7	4
173	Monte Carlo modeling of transient recharging processes in quantum-well infrared photodetectors. IEEE Transactions on Electron Devices, 2000, 47, 1935-1942.	3.0	9
174	Periodic electric-field domains in optically excited multiple-quantum-well structures. Physical Review B, 2000, 61, 2742-2748.	3.2	26
175	Phenomenological theory of electric-field domains induced by infrared radiation in multiple quantum well structures. Physical Review B, 2000, 62, 7268-7274.	3.2	20
176	Nonlinear dynamics of recharging processes in multiple quantum well structures excited by infrared radiation. Physical Review B, 2000, 62, 10292-10296.	3.2	10
177	Modeling of the terahertz response of metal-semiconductor-metal photodetectors. , 1999, , .		0
178	Theoretical Study of Recharging Instability in Quantum Well Infrared Photodetectors. Japanese Journal of Applied Physics, 1999, 38, 6654-6658.	1.5	8
179	Effect of Donor Space Charge on Electron Capture Processes in Quantum Well Infrared Photodetectors. Japanese Journal of Applied Physics, 1999, 38, 6650-6653.	1.5	16
180	Recharging Instability and Periodic Domain Structures in Multiple Quantum Well Infrared Photodetectors. Japanese Journal of Applied Physics, 1999, 38, L1388-L1390.	1.5	13

#	Article	IF	CITATIONS
181	Monte Carlo Modeling of Electron Transport and Capture Processes in AlGaAs/GaAs Multiple Quantum Well Infrared Photodetectors. Japanese Journal of Applied Physics, 1999, 38, 5922-5927.	1.5	29
182	Impact of transit-time and capture effects on high-frequency performance of multiple quantum-well infrared photodetectors. IEEE Transactions on Electron Devices, 1998, 45, 293-298.	3.0	26
183	Capture and transit-time electron effects in high-frequency operation of multiple quantum well infrared photodetectors. Physica E: Low-Dimensional Systems and Nanostructures, 1998, 2, 142-145.	2.7	2
184	Monte Carlo modeling of electron velocity overshoot effect in quantum well infrared photodetectors. Journal of Applied Physics, 1998, 84, 3403-3408.	2.5	29
185	High-Frequency Response of Metal-Semiconductor-Metal Photodetectors Limited by Dynamic and Recombination Effects. Japanese Journal of Applied Physics, 1998, 37, 6352-6357.	1.5	5
186	Influence of Electron Velocity Overshoot Effect on High-Frequency Characteristics of Quantum Well Infrared Photodetectors. Japanese Journal of Applied Physics, 1998, 37, 78-83.	1.5	10
187	Terahertz response of metal-semiconductor-metal photodetectors. Journal of Applied Physics, 1998, 84, 6419-6425.	2.5	7
188	Monte Carlo analysis of ultrafast electron transport in quantum well infrared photodetectors. Applied Physics Letters, 1998, 72, 842-844.	3.3	37
189	Optically Controlled Plasma Resonances in Induced-Base Hot-Electron Transistors. Japanese Journal of Applied Physics, 1997, 36, 5472-5474.	1.5	6
190	Monte Carlo Modeling of Transient Effects in Resonant-Tunneling Bipolar Transistors. Japanese Journal of Applied Physics, 1997, 36, 5060-5062.	1.5	2
191	Heterostructure laser-transistors controlled by resonant-tunnelling electron extraction. Semiconductor Science and Technology, 1997, 12, 431-438.	2.0	4
192	High-Frequency Response of Intersubband Infrared Photodetectors with a Multiple Quantum Well Structure. Japanese Journal of Applied Physics, 1997, 36, 2596-2600.	1.5	15
193	Analysis of integrated quantum-well infrared photodetector and light-emitting diode for implementing pixelless imaging devices. IEEE Journal of Quantum Electronics, 1997, 33, 1527-1531.	1.9	40
194	Optimisation of bistable quantum well IR phototransistors. IEE Proceedings: Optoelectronics, 1997, 144, 283-286.	0.8	1
195	Multiple quantum-dot infrared phototransistors. Physica B: Condensed Matter, 1996, 227, 17-20.	2.7	13
196	Injection Lasers With a Resonant-Tunneling Controlling Structure. , 1996, , .		0
197	Resonant-Tunneling Bipolar Transistors with a Quantum-Well Base. Japanese Journal of Applied Physics, 1996, 35, 5280-5283.	1.5	3
198	Comparison Studies of Infrared Phototransistors with a Quantum-Well and a Quantum-Wire Base. European Physical Journal Special Topics, 1996, 06, C3-157-C3-161.	0.2	11

#	Article	IF	CITATIONS
199	Fast Modulation of a Laser-Phototransistor by Long-Wavelength Infrared Radiation. , 1996, , 615-617.		Ο
200	Theoretical study of an infrared-to-visible wavelength quantum-well converter. Semiconductor Science and Technology, 1995, 10, 1272-1276.	2.0	5
201	Quantum Well Infrared Photodetector with Optical Output. Japanese Journal of Applied Physics, 1995, 34, L38-L40.	1.5	23
202	Modeling of Lateral Hot-Electron Phototransistor for Long-Wave Length Infrared Radiation. Japanese Journal of Applied Physics, 1995, 34, 206.	1.5	1
203	Intersubband infrared phototransistors with a quantum-wire base. , 0, , .		Ο
204	Limits Of Ultrahigh-speed Operation Of Quantum-well Infrared Photodetectors. , 0, , .		0
205	Monte Carlo particle modeling of electron velocity overshoot effect in MSM photodiodes. , 0, , .		0
206	Terahertz operation of GaAs/AlGaAs metal-semiconductor-metal photodetectors. , 0, , .		0
207	Terahertz response of MSM photodiodes: Monte Carlo simulation. , 0, , .		Ο
208	Monte Carlo simulation of terahertz response of MSM photodetectors. , 0, , .		0
209	Self-organization and pulsing in multiple quantum well structures excited by infrared radiation. , 0, , .		0
210	Physical model and characteristics of quantum dot infrared photodetectors. , 0, , .		0
211	Modeling of the excitation of terahertz plasma oscillations in a HEMT by ultrashort optical pulses. , 0, , .		1
212	Device Model for Graphene Nanoribbon Phototransistor. Applied Physics Express, 0, 1, 063002.	2.4	76
213	Graphene Tunneling Transit-Time Terahertz Oscillator Based on Electrically Induced p–i–n Junction. Applied Physics Express, 0, 2, 034503.	2.4	45
214	Coulomb Drag by Injected Ballistic Carriers in Graphene n + â~'iâ~'nâ~'n + Structures: Doping and Temperature Effects. Physica Status Solidi (A) Applications and Materials Science, 0, , 2100535.	1.8	3
215	Simulation of ectopic activity onset in border zones between normal and damaged myocardium with minimal ionic models. , 0, , .		2
216	Ballistic Injection Terahertz Plasma Instability in Graphene n + ―i – n – n + Fieldâ€Effect Transistors and Lateral Diodes. Physica Status Solidi (A) Applications and Materials Science, 0, , .	1.8	6